

Magnetization Switching of a Co/Pt Multilayered Perpendicular Nanomagnet Assisted by a Microwave Field with Time-Varying Frequency

Hirofumi Suto,* Taro Kanao, Tazumi Nagasawa, Koichi Mizushima, and Rie Sato
*Corporate Research and Development Center, Toshiba Corporation, 1 Komukai-Toshiba-cho,
 Saiwai-ku, Kawasaki 212-8582, Japan*

 (Received 12 September 2017; revised manuscript received 27 March 2018; published 8 May 2018)

Microwave-assisted magnetization switching (MAS) is attracting attention as a method for reversing nanomagnets with a high magnetic anisotropy by using a small-amplitude magnetic field. We experimentally study MAS of a perpendicularly magnetized nanomagnet by applying a microwave magnetic field with a time-varying frequency. Because the microwave field frequency can follow the nonlinear decrease of the resonance frequency, larger magnetization excitation than that in a constant-frequency microwave field is induced, which enhances the MAS effect. The switching field decreases almost linearly as the start value of the time-varying microwave field frequency increases, and it becomes smaller than the minimum switching field in a constant-frequency microwave field. To obtain this enhancement of the MAS effect, the end value of the time-varying microwave field frequency needs to be almost the same as or lower than the critical frequency for MAS in a constant-frequency microwave field. In addition, the frequency change typically needs to take 1 ns or longer to make the rate of change slow enough for the magnetization to follow the frequency change. This switching behavior is qualitatively explained by the theory based on the macrospin model.

DOI: [10.1103/PhysRevApplied.9.054011](https://doi.org/10.1103/PhysRevApplied.9.054011)

I. INTRODUCTION

Magnetization switching that utilizes ferromagnetic resonance (FMR) excitation has attracted attention as a write method in next-generation magnetic recording [1–20]. To date, experimental studies on this kind of magnetization switching have employed a microwave field with a time-constant frequency and have shown that the switching field of a nanomagnet substantially decreases by applying a microwave field with a frequency on the order of the FMR frequency of the nanomagnet [5]. This switching method is called microwave-assisted magnetization switching (MAS). Furthermore, magnetization switching induced solely by a circularly polarized microwave field has been proposed and experimentally demonstrated [10,11]. FMR is a nonlinear phenomenon and the resonance frequency at which the magnetization excitation becomes largest depends on the amplitude of the magnetization excitation. Because the FMR-based magnetization switching methods utilize large magnetization excitation, nonlinearity plays an important role and needs to be taken into account to explain the switching behavior [12–14]. At the same time, the nonlinearity of FMR suggests that a microwave field with a time-varying frequency can induce larger magnetization excitation than a microwave field with a time-constant frequency. Regarding nanomagnets with perpendicular

magnetic anisotropy, which are of interest in high-density magnetic recording applications, the resonance frequency decreases as the amplitude of the magnetization excitation evolves. Therefore, by gradually decreasing the frequency of the microwave field, the nonlinear decrease of the resonance frequency can be followed and the magnetization excitation can be enhanced. Theoretical and micromagnetic simulation studies have reported that this kind of microwave field can efficiently induce magnetization switching [15–19]. However, no experimental studies have yet been reported.

In magnetic recording applications, it has been proposed that a spin-torque oscillator (STO) can be used as a microwave field source [21,22]. One way to realize a varying-frequency microwave field is to change the current injected into the STO [17]. Furthermore, it has been reported that, in a certain geometry, the STO spontaneously changes the frequency during the switching process because of the interaction with the media magnetization [19].

In this paper, we experimentally study magnetization switching of a Co/Pt nanomagnet with perpendicular magnetic anisotropy by applying a microwave field with a time-varying frequency and compare the switching behavior to that in a microwave field with a constant frequency. For convenience, we introduce the following symbols for microwave field frequency (f_{rf}). In constant-frequency MAS (CF MAS), the microwave field frequency is constant and is referred to as $f_{\text{rf}}^{\text{const}}$. In varying-frequency

*hirofumi.suto@toshiba.co.jp

MAS (VF MAS), the start and end values of the time-varying microwave field frequency are referred to as $f_{\text{rf}}^{\text{start}}$ and $f_{\text{rf}}^{\text{end}}$, respectively. In CF MAS, the switching field of the nanomagnet decreases almost linearly with an increasing $f_{\text{rf}}^{\text{const}}$ value, reaches a minimum at the critical frequency, and then increases abruptly. In VF MAS, the switching field similarly decreases linearly with increasing an $f_{\text{rf}}^{\text{start}}$ value but continues to decrease even when $f_{\text{rf}}^{\text{start}}$ becomes higher than the critical frequency for CF MAS. The switching field thus becomes lower than the minimum switching field for CF MAS, showing that the MAS effect is enhanced by a microwave field with varying frequency. To obtain this enhancement of the MAS effect, $f_{\text{rf}}^{\text{end}}$ needs to be almost the same as or lower than the critical frequency for CF MAS. In addition, the f_{rf} change needs to take approximately 1 ns or longer when $f_{\text{rf}}^{\text{end}}$ is set to half of $f_{\text{rf}}^{\text{start}}$ to make the rate of f_{rf} change sufficiently slow. The switching behavior of VF MAS can be explained qualitatively by the theory that describes the magnetization dynamics of a single spin in a microwave magnetic field.

II. SAMPLE STRUCTURE AND EXPERIMENTAL SETUP

Figure 1(a) shows the sample structure and the measurement setup. A Ta bottom layer and Co/Pt multilayer magnetic film are deposited on a sapphire substrate by using a magnetron sputtering system. The film structure from bottom to top is Ta 200/Pt 50/(Co 13.6/Pt 5) \times 5/Pt 50/Ta 50 (thicknesses are given in angstroms). Figure 1(b) shows magnetization as a function of the z -direction magnetic field (H_z) measured by using a vibrating sample magnetometer. The average saturation magnetization (M_s) of the Co/Pt film is estimated to be 1200 emu/cm³, assuming that the total thickness of the magnetic layer is from the bottommost Co layer to the topmost Co layer. Figure 1(c) shows vector network analyzer (VNA)-FMR spectra of the film sample as a function of H_z . At around $H_z = 0$ Oe, the FMR peak disappears because of the formation of reversed magnetic domains, and the FMR frequency at $H_z = 0$ Oe is estimated to be 5 GHz by linear extrapolation. This FMR frequency indicates that the effective perpendicular anisotropy field ($H_{\text{ani}}^{\text{eff}}$) of the film, including the demagnetizing field, is approximately 1.8 kOe, and the perpendicular anisotropy field (H_{ani}) is estimated to be 16.9 kOe from $H_{\text{ani}} = H_{\text{ani}}^{\text{eff}} + 4\pi M_s$. Figure 1(d) shows the linewidth of the FMR absorption peak (Δf_{FMR}) as a function of the resonance frequency (f_{FMR}) obtained in the H_z range from -2.4 to -0.8 kOe. This relationship can be expressed as $\Delta f_{\text{FMR}} = 2\alpha f_{\text{FMR}} + \Delta f_0$, where Δf_0 denotes linewidth broadening due to the film inhomogeneity. From the fitting, the damping parameter (α) of the film is estimated to be 0.035.

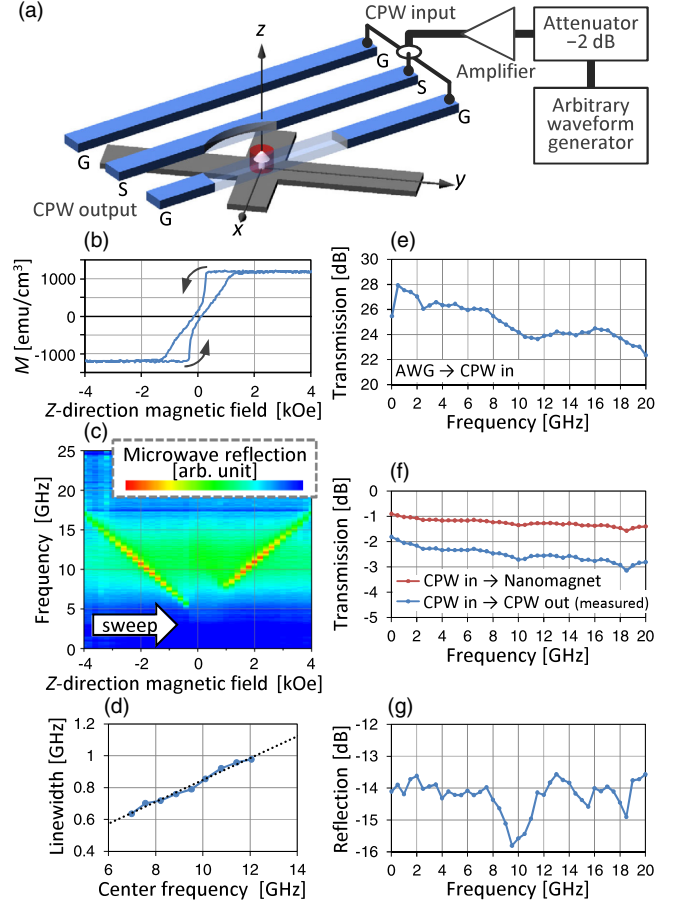


FIG. 1. (a) Sample structure and experimental setup. (b) M - H_z loop obtained for the film sample having an area of 1 cm². (c) VNA-FMR spectra versus H_z obtained for the film sample. (d) Linewidth of the FMR absorption peak versus FMR frequency. The dotted line depicts the linear fit. (e) Microwave transmission between the cable end connected to the AWG and the cable end connected to the CPW input. (f) Microwave transmission between the input and output of the CPW. Half of the measured value is employed as microwave transmission between the CPW input and above the nanomagnet. (g) Microwave reflection at the CPW input.

The Co/Pt film is then patterned into a nanomagnet with a diameter of 50 nm by electron-beam lithography and Ar ion milling. The Ta bottom layer is patterned into a Hall cross to detect switching of the nanomagnet by the anomalous Hall effect. After that, insulating layers of 20-nm-thick SiN and 80-nm-thick SiO₂ are sputter deposited, and a coplanar waveguide (CPW) made of 100-nm-thick Cu with thin adhesion layers is fabricated. The signal line of the CPW passes above the nanomagnet with a separation of 100 nm. The widths of the CPW signal (S) line, ground (G) lines, and gaps are 1, 2, and 2 μm above the nanomagnet and gradually expand to 80, 80, and 45 μm at the contact pads. These dimensions are chosen to make the characteristic impedance roughly 50 Ω , as calculated by using AppCAD software. Note that the CPW dimensions are the design values, and the actual

dimensions deviate from them and have a tapered cross section. The length of the CPW is $750 \mu\text{m}$. This length is approximately one tenth of the wavelength of microwave signal traveling through the CPW at 16 GHz, which is the highest in the studied frequency range. A transmission-electron-microscopy image of the nanomagnet that has a slightly different Co thickness but is fabricated using the same process is provided in Ref. [9].

We study switching of the nanomagnet by applying H_z and an in-plane microwave magnetic field from the CPW. When no microwave field is applied, the switching z -direction dc magnetic field (H_{sw}) of the nanomagnet is 5.7 kOe. Hereafter, this value is referred to as the intrinsic H_{sw} . To generate a microwave field, a microwave signal is generated from a Keysight M8195A arbitrary waveform generator (AWG) with a 64-GHz sampling rate, amplified by an RF-LAMBDA RFLUPA00G22GA wide-band amplifier, and introduced to the CPW. The amplifier has a bandwidth of 0.02–22 GHz, an average gain of +30 dB, and a gain flatness of ± 2.5 dB. Figure 1(e) shows the microwave transmission between the cable end connected to the AWG and the cable end connected to the input of the CPW, as measured by the VNA. The variation from +22 to +28 dB is due to the frequency dependence of the gain of the amplifier and the attenuation of the cables. The microwave property of the CPW is also evaluated. Figure 1(f) shows the microwave transmission between the input and the output of the CPW. The attenuation ranges from -2 to -3 dB. The microwave reflection at the CPW input [Fig. 1(g)] is approximately -14 dB, showing that there is no severe reflection point, such as a large impedance mismatch. Considering that the phase of the reflection is close to 0° (data not shown), the characteristic impedance of the CPW is estimated to be approximately 75Ω . In this estimation, multiple reflection in the CPW is neglected. In addition, the CPW is shorter than one tenth of the wavelength; thus, impedance mismatch has a small effect on the microwave transmission. We employ the sum of the microwave transmission from the AWG to the CPW input and half of the microwave transmission of the CPW as the microwave transmission from the AWG to above the nanomagnet because the nanomagnet is located below the middle of the CPW. This calculated microwave transmission is used to construct the waveform of the AWG.

The microwave field amplitude (H_{rf}) generated from the CPW is estimated by using the Biot-Savart formula assuming a uniform current in the signal line. In this estimation, the tapered cross section of the CPW observed by transmission electron microscopy is considered. When a microwave signal with a voltage (V_{rf}) of 1 V travels above the nanomagnet, a microwave field with $H_{\text{rf}} = 85$ Oe is applied. The microwave signal is modulated into pulses of nanosecond-order duration to avoid heating the sample and is emitted repeatedly from the AWG at 122 kHz.

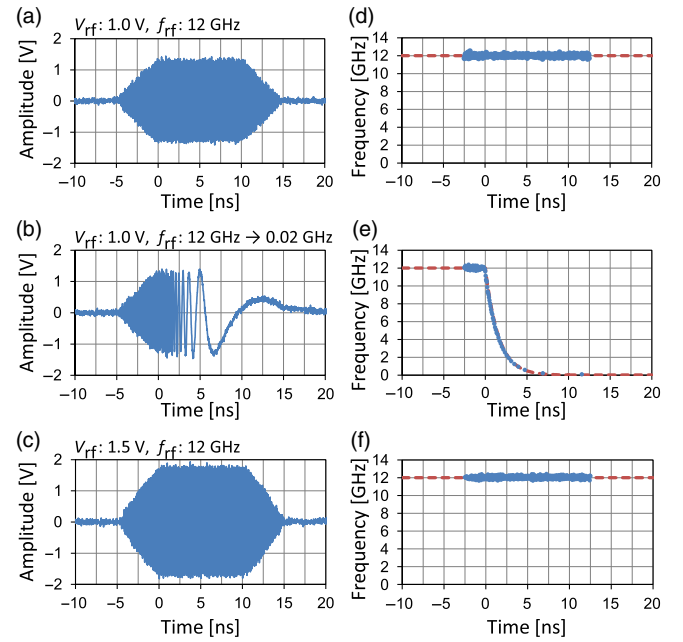


FIG. 2. (a)–(c) Waveforms of signals for the following parameter sets: ($V_{\text{rf}} = 1.0 \text{ V}$, $f_{\text{rf}}^{\text{const}} = 12 \text{ GHz}$), ($V_{\text{rf}} = 1.0 \text{ V}$, $f_{\text{rf}}^{\text{start}} = 12 \text{ GHz}$, $f_{\text{rf}}^{\text{end}} = 0.02 \text{ GHz}$), and ($V_{\text{rf}} = 1.5 \text{ V}$, $f_{\text{rf}}^{\text{const}} = 12 \text{ GHz}$). These waveforms are measured at the cable end connected to the CPW input, and the amplitude further attenuates by half of the microwave transmission in Fig. 1(f) when above the nanomagnet. Because this attenuation is from -1 to -1.5 dB, the signal amplitude becomes 89% to 84% of the measured voltage. (d)–(f) Instantaneous f_{rf} values estimated from the zero-cross intervals of the waveforms. Each dot corresponds to one zero-cross interval. The dots overlap the designed f_{rf} depicted by dashed lines.

Figure 2(a) shows the waveform of a constant-frequency microwave signal that has a 5-ns rise and fall time, a 10-ns plateau time, $V_{\text{rf}} = 1.0 \text{ V}$, and $f_{\text{rf}}^{\text{const}} = 12 \text{ GHz}$. The rise and fall times are fixed to 5 ns throughout the experiments, and the plateau time is 10 ns except when the plateau time dependence is measured in Sec. III D. The measured voltage is larger than 1 V because this signal waveform is measured by disconnecting the cable end from the CPW input and connecting it to an oscilloscope with an 80-GHz sampling rate. The signal amplitude, therefore, further attenuates by half of the microwave transmission in Fig. 1(f) and becomes almost 1 V above the nanomagnet. Figure 2(d) shows the instantaneous f_{rf} estimated from the zero-cross intervals of the waveform, which confirms that f_{rf} is actually 12 GHz. Similarly, a varying-frequency microwave signal is generated that takes into account the frequency dependence of the microwave transmission. Figure 2(b) shows the waveform of a varying-frequency microwave signal with $V_{\text{rf}} = 1.0 \text{ V}$, $f_{\text{rf}}^{\text{start}} = 12 \text{ GHz}$, and $f_{\text{rf}}^{\text{end}} = 0.02 \text{ GHz}$. During the rise and fall time, f_{rf} is constant and, during the plateau time, f_{rf} decreases. The signal amplitude is almost the same as that with the

constant frequency [Fig. 2(a)], although it fluctuates because the frequency-dependent microwave transmission is not perfectly compensated for. Regarding the f_{rf} change, we think that the rate of f_{rf} change should be faster when f_{rf} is higher because it takes a shorter time for a microwave field to induce magnetization excitation when f_{rf} is higher. To realize such an f_{rf} change, we employ the following function:

$$f_{\text{rf}}(t) = f_{\text{rf}}^{\text{start}} \exp\left(-\frac{t}{t_{\text{plateau}}} \ln \frac{f_{\text{rf}}^{\text{start}}}{f_{\text{rf}}^{\text{end}}}\right), \quad (1)$$

where t_{plateau} denotes the plateau time. This function is derived from $df_{\text{rf}}/dt \propto f_{\text{rf}}$, where the rate of f_{rf} change is proportional to f_{rf} . This function is one example of f_{rf} change, and further study is necessary to optimize f_{rf} change for efficient MAS. Note that Ref. [15] reported a function in which f_{rf} always matches the resonance frequency when α is small. Figure 2(e) shows the estimated instantaneous f_{rf} of the waveform in Fig. 2(b), which confirms that f_{rf} changes as designed. Figures 2(c) and 2(f) show a constant-frequency signal waveform with $V_{\text{rf}} = 1.5$ V and $f_{\text{rf}}^{\text{const}} = 12$ GHz and the instantaneous f_{rf} , which we mention later in the next section.

III. EXPERIMENTAL RESULTS

A. Comparison between constant-frequency MAS and varying-frequency MAS, and effect of the start frequency on varying-frequency MAS

In this section, we first study switching of the nanomagnet in a constant-frequency microwave field, then apply a varying-frequency microwave field to study the effect of $f_{\text{rf}}^{\text{start}}$.

Figure 3(a) shows the dependence of H_{sw} on $f_{\text{rf}}^{\text{const}}$ for CF MAS. These data and this kind of frequency dependence of H_{sw} , as shown later in this paper, are measured as follows: at each frequency, the nanomagnet is initialized to the $-z$ direction, and H_z is increased in steps of 10 Oe per 0.3 s until magnetization switching is detected. During this H_z increase, a pulsed microwave field is applied repeatedly. Each curve in Fig. 3(a) is obtained by setting V_{rf} to 0.5–2.0 V, which generates H_{rf} of 43–170 Oe. As $f_{\text{rf}}^{\text{const}}$ increases, H_{sw} decreases almost linearly until H_{sw} takes a minimum at the critical frequency, then H_{sw} increases abruptly to the intrinsic H_{sw} of 5.7 kOe. This kind of switching behavior has been reported by previous experimental studies on MAS [5], which can be understood as follows. When H_z is applied in the opposite direction to the magnetization, the FMR frequency decreases. Therefore, the resonance condition in which the FMR frequency is near $f_{\text{rf}}^{\text{const}}$ results in a $H_{\text{sw}} - f_{\text{rf}}^{\text{const}}$ curve with a negative slope. However, when $f_{\text{rf}}^{\text{const}}$ becomes higher than the critical frequency, matching H_z becomes so small that a microwave field cannot induce magnetization excitation

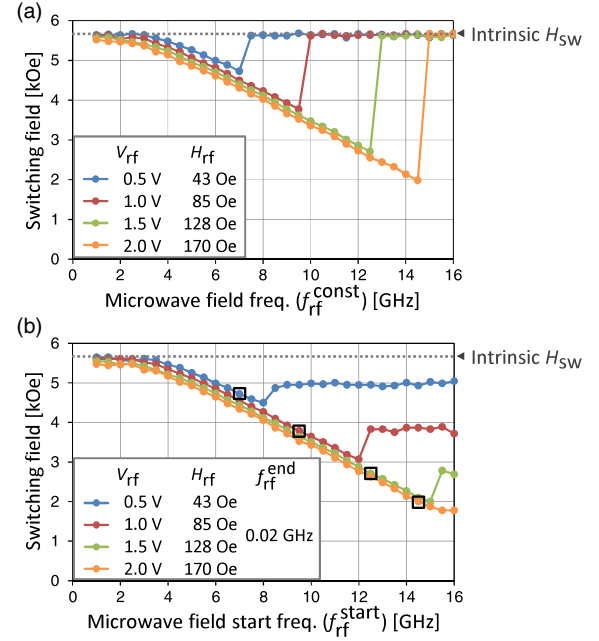


FIG. 3. (a) H_{sw} versus $f_{\text{rf}}^{\text{const}}$ for CF MAS. (b) H_{sw} versus $f_{\text{rf}}^{\text{start}}$ for VF MAS obtained by setting $f_{\text{rf}}^{\text{end}} = 0.02$ GHz. Squares show the corresponding critical frequency and H_{sw} for CF MAS.

large enough to induce magnetization switching. As H_{rf} increases, the critical frequency increases and the corresponding H_{sw} decreases, showing that a larger MAS effect is obtained by applying a microwave field with a larger H_{rf} value.

Figure 3(b) shows the dependence of H_{sw} on $f_{\text{rf}}^{\text{start}}$ for VF MAS. To focus on the effect of $f_{\text{rf}}^{\text{start}}$, $f_{\text{rf}}^{\text{end}}$ is set as low as 0.02 GHz. When $f_{\text{rf}}^{\text{start}}$ is smaller than the critical frequency of CF MAS, the H_{sw} versus $f_{\text{rf}}^{\text{start}}$ curves almost coincide with the H_{sw} versus $f_{\text{rf}}^{\text{const}}$ curves for CF MAS. This coincidence indicates that magnetization switching in the varying-frequency microwave field occurs in the same manner as CF MAS because the frequencies of the two kinds of microwave field are almost the same at the beginning of the f_{rf} change. When $f_{\text{rf}}^{\text{start}}$ becomes higher than the critical frequency, H_{sw} continues to decrease and becomes smaller than the minimum value for CF MAS, showing that the MAS effect is enhanced. We now confirm that this enhancement of the MAS effect actually originates from the varying-frequency microwave field by examining the waveform of the microwave signals. In VF MAS, H_{sw} for $V_{\text{rf}} = 1.0$ V decreases to 3.05 kOe at $f_{\text{rf}}^{\text{start}} = 12$ GHz. In CF MAS, no MAS effect is obtained for $V_{\text{rf}} = 1.0$ V at $f_{\text{rf}}^{\text{const}} = 12$ GHz because $f_{\text{rf}}^{\text{const}}$ is above the critical frequency, and the MAS effect is obtained by increasing V_{rf} to 1.5 V, where the critical frequency is at 12.5 GHz. Waveforms of these signals are shown in Figs. 2(a), 2(b), and 2(c). The amplitude of the varying-frequency microwave signal for $V_{\text{rf}} = 1.0$ V [Fig. 2(b)] is clearly

smaller than that of the constant-frequency microwave signal for $V_{\text{rf}} = 1.5$ V [Fig. 2(c)]. The fact that these two signals achieve almost the same MAS effect is evidence that the enhancement in the MAS effect is due to the varying-frequency microwave field.

As $f_{\text{rf}}^{\text{start}}$ increases, the H_{sw} curves for $V_{\text{rf}} = 0.5, 1.0,$ and 1.5 V take the minimum and increase abruptly. For $V_{\text{rf}} = 2.0$ V, such an abrupt H_{sw} increase does not appear, probably because its frequency is above 16 GHz. This abrupt increase in H_{sw} cannot be explained by considering only f_{rf} . For example, H_{sw} for $V_{\text{rf}} = 1.0$ V and $f_{\text{rf}}^{\text{start}} = 12$ GHz (below the abrupt increase) is smaller than that for $V_{\text{rf}} = 1.0$ V and $f_{\text{rf}}^{\text{start}} = 12.5$ GHz (above the abrupt increase), which is inconsistent with the fact that the f_{rf} change for $f_{\text{rf}}^{\text{start}} = 12.5$ GHz passes through 12 GHz and decreases to $f_{\text{rf}}^{\text{end}} = 0.02$ GHz. The fact that the VF-MAS result cannot be explained by considering only f_{rf} indicates that the rate of f_{rf} change needs to be taken into account as follows. When $f_{\text{rf}}^{\text{start}}$ is too high, the rate of f_{rf} change becomes too fast for the magnetization excitation to follow. As a result, the varying-frequency microwave field can no longer enhance the MAS effect. Above the abrupt increase, H_{sw} becomes approximately the same as H_{sw} at the critical frequency for CF MAS. This result indicates that magnetization switching occurs in the same manner as CF MAS when f_{rf} decreases and matches the critical frequency for CF MAS.

B. Effect of the end frequency on varying-frequency MAS

We next examine the effect of $f_{\text{rf}}^{\text{end}}$ on VF MAS. As shown in the previous section, enhancement of the MAS effect is not apparent for $V_{\text{rf}} = 2.0$ V because the critical frequency is already close to the upper limit of the studied frequency range. Thus, we show the results for $V_{\text{rf}} = 0.5, 1.0,$ and 1.5 V. We fix $f_{\text{rf}}^{\text{start}}$ to 8, 12, and 15 GHz, respectively, for $V_{\text{rf}} = 0.5, 1.0,$ and 1.5 V, at which H_{sw} takes the minimum in Fig. 3(b), and $f_{\text{rf}}^{\text{end}}$ is varied. Figures 4(a)–4(d) show the waveforms and estimated instantaneous f_{rf} values of signals with $V_{\text{rf}} = 1.0$ V, $f_{\text{rf}}^{\text{start}} = 12$ GHz, and $f_{\text{rf}}^{\text{end}} = 1$ and 11 GHz, respectively, which confirms that the signals have the designed amplitude and frequency regardless of the amount of f_{rf} change. Figure 4(e) shows the dependence of H_{sw} on $f_{\text{rf}}^{\text{end}}$. As already shown in the previous section, H_{sw} becomes smaller than H_{sw} at the critical frequency for CF MAS when $f_{\text{rf}}^{\text{end}} = 0.02$ GHz because the varying-frequency microwave field enhances the MAS effect. As $f_{\text{rf}}^{\text{end}}$ increases, H_{sw} is first constant and then abruptly increases to the intrinsic H_{sw} , showing that the MAS effect disappears when $f_{\text{rf}}^{\text{end}}$ is too high. Waveforms of the signals for $f_{\text{rf}}^{\text{end}}$ below and above the abrupt H_{sw} increase [Figs. 4(a) and 4(b)] confirm that this drastic change of the switching behavior originates from the different $f_{\text{rf}}^{\text{end}}$ value. The

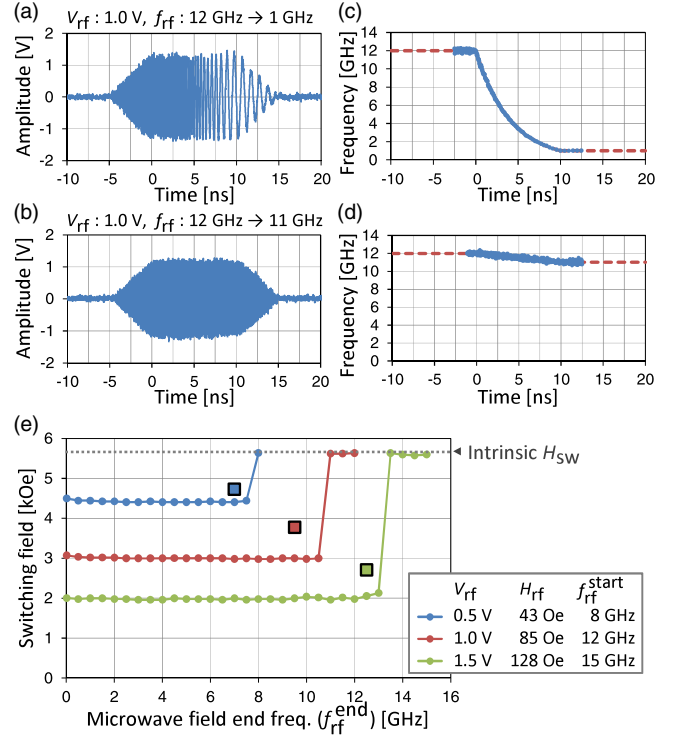


FIG. 4. (a),(b) Waveforms of signals for the following parameter sets: ($V_{\text{rf}} = 1.0$ V, $f_{\text{rf}}^{\text{start}} = 12$ GHz, $f_{\text{rf}}^{\text{end}} = 1$ GHz) and ($V_{\text{rf}} = 1.0$ V, $f_{\text{rf}}^{\text{start}} = 12$ GHz, $f_{\text{rf}}^{\text{end}} = 11$ GHz). (c),(d) Instantaneous f_{rf} values estimated from the zero-cross intervals of the waveforms. (e) H_{sw} versus $f_{\text{rf}}^{\text{end}}$ for VF MAS obtained by setting $f_{\text{rf}}^{\text{start}} = 8, 12,$ and 15 GHz, respectively, for $V_{\text{rf}} = 0.5, 1.0,$ and 1.5 V. Squares show the corresponding critical frequency and H_{sw} for CF MAS.

frequency at which H_{sw} increases is almost the same as the corresponding critical frequency. This result shows that $f_{\text{rf}}^{\text{end}}$ needs to be approximately the same as or lower than the critical frequency for CF MAS to enhance the MAS effect by applying a varying-frequency microwave field.

C. Minimizing the switching field by applying a varying-frequency microwave field

In Sec. III A, the H_{sw} curves for VF MAS exhibit the abrupt increase because the rate of f_{rf} change becomes too fast. This result suggests that H_{sw} can be even smaller when the rate of f_{rf} change is sufficiently slow. To determine the minimum H_{sw} that can be achieved by VF MAS, we again measure the dependence of H_{sw} on $f_{\text{rf}}^{\text{start}}$. In Sec. III B, it is found that $f_{\text{rf}}^{\text{end}}$ needs to be almost the same as or lower than the critical frequency for CF MAS. Based on this finding, $f_{\text{rf}}^{\text{end}}$ is set to the critical frequencies of 7, 9.5, and 12.5 GHz, respectively, for $V_{\text{rf}} = 0.5, 1.0,$ and 1.5 V. As shown in Fig. 5, H_{sw} gradually decreases with an increasing $f_{\text{rf}}^{\text{start}}$ value, then H_{sw} becomes almost constant with no abrupt increase. This constant H_{sw} value means that magnetization switching occurs in the same manner in this

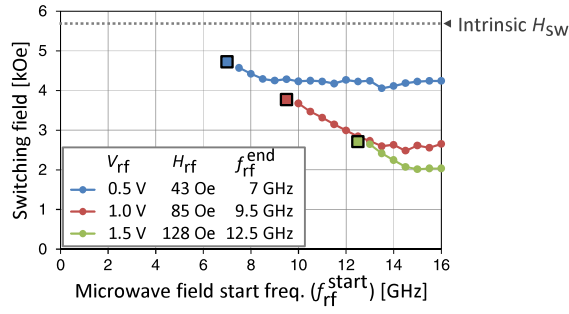


FIG. 5. H_{sw} versus f_{rf}^{start} for VF MAS obtained by setting $f_{rf}^{end} = 7, 9.5,$ and 12.5 GHz, respectively, for $V_{rf} = 0.5, 1.0,$ and 1.5 V. Squares show the corresponding critical frequency and H_{sw} for CF MAS.

f_{rf}^{start} range because the f_{rf} change for a certain f_{rf}^{start} passes through the f_{rf} change for a lower f_{rf}^{start} value. The constant H_{sw} also means that the rate of f_{rf} change is sufficiently slow. Therefore, the obtained H_{sw} value is considered to be the minimum that can be achieved by VF MAS. The difference between the minimum H_{sw} value for CF and VF MAS is the largest for $V_{rf} = 1.0$ V, followed by 1.5 and 0.5 V, showing that a varying-frequency microwave field can enhance the MAS effect most efficiently for a certain H_{rf} . This H_{rf} dependence is theoretically discussed in Sec. IV.

D. Effect of rate of change in microwave field frequency

In this section, we study the effect of the rate of f_{rf} change by varying $t_{plateau}$. We set f_{rf}^{start} to 8, 12, and 15 GHz, respectively, for $V_{rf} = 0.5, 1.0,$ and 1.5 V, which are used for measuring the f_{rf}^{end} dependence [Fig. 4(e)], and we set f_{rf}^{end} to half of f_{rf}^{start} . Figures 6(a) and 6(b) show the waveform and estimated instantaneous f_{rf} values of a signal with $V_{rf} = 1.0$ V, $f_{rf}^{start} = 12$ GHz, $f_{rf}^{end} = 6$ GHz, and $t_{plateau} = 2$ ns, which confirms that the signal has the designed amplitude and frequency even for the short $t_{plateau}$. Figure 6(c) shows the dependence of H_{sw} on $t_{plateau}$. When $t_{plateau}$ is 2 ns, H_{sw} is the same as that for the slow f_{rf} change [Fig. 5], showing that the rate of f_{rf} change is sufficiently slow at 2 ns. As $t_{plateau}$ decreases, H_{sw} is first constant and then increases abruptly. This increase appears at $t_{plateau} = 1.0$ – 1.2 ns, depending on V_{rf} . Below these $t_{plateau}$ values, the rate of f_{rf} change becomes too fast and the enhancement of the MAS effect disappears. Immediately after this abrupt increase, H_{sw} becomes almost the same as H_{sw} at the critical frequency for CF MAS. In this condition, magnetization switching occurs in the same manner as CF MAS when f_{rf} decreases to the critical frequency, as already discussed in Sec. III A. As $t_{plateau}$ further decreases, H_{sw} gradually increases. This $t_{plateau}$ dependence is explained as follows. As the rate of f_{rf} change becomes faster, the time duration in which f_{rf} is

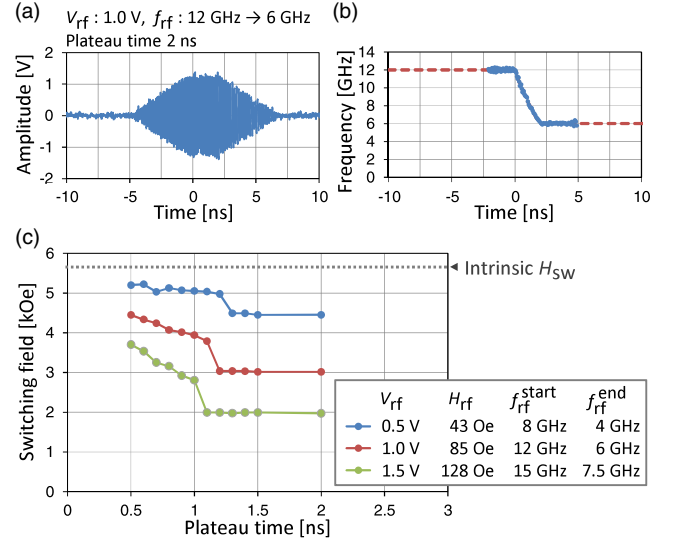


FIG. 6. (a),(b) Waveform and instantaneous f_{rf} of a signal with $V_{rf} = 1.0$ V, $f_{rf}^{start} = 12$ GHz, $f_{rf}^{end} = 6$ GHz, and $t_{plateau} = 2$ ns. (c) H_{sw} versus $t_{plateau}$ for VF MAS obtained by setting $f_{rf}^{end} = f_{rf}^{start}/2$.

near the critical frequency becomes shorter. Because the magnetization excitation is still developing on this time-scale, the MAS effect weakens, and thus H_{sw} increases.

IV. THEORY OF MAGNETIZATION SWITCHING IN A VARYING-FREQUENCY MICROWAVE FIELD BASED ON THE MACROSPIN MODEL

The magnetization dynamics of a single spin in a rotating microwave field can be described by the Landau-Lifshitz-Gilbert (LLG) equation formulated in a rotating frame, and the switching condition can be derived by examining the stability of the steady-state solutions of the LLG equation [12]. Although issues such as spatially nonuniform magnetization excitation [6], a quasiperiodic magnetization motion [12], and thermally activated magnetization switching [14] are not accounted for, it is known that the switching behavior of CF MAS is qualitatively reproduced by this approach. In this section, we explain the switching behavior of VF MAS using this approach. We employ the following normalization, which is applicable to magnetization with uniaxial anisotropy, regardless of the strength of the anisotropy field. The rotating microwave field and z -direction dc magnetic field are normalized in units of the anisotropy field (H_{ani}): $h_{rf} = H_{rf}^{rot}/H_{ani}$, $h_z = H_z/H_{ani}$. Note that H_{rf}^{rot} here means the amplitude of the rotating microwave field, whereas H_{rf} in the experiments means the amplitude of the microwave field alternating in one direction. It has been reported that a rotating microwave field induces the same MAS effect at half the microwave field amplitude compared to an alternating microwave magnetic field [8,9]. This is the case because an alternating

microwave field is decomposed into two rotating microwave fields that rotate in the opposite direction and have half the amplitude, and only the rotating microwave field that rotates in the same direction as the FMR precession induces magnetization excitation. The microwave field frequency is normalized in units of FMR frequency: $\omega_{\text{rf}} = (2\pi f_{\text{rf}})/(\gamma H_{\text{ani}})$, where γ denotes the gyromagnetic ratio. Similarly, time is normalized as $\tau = t(\gamma H_{\text{ani}})$. The LLG equation that describes the dynamics of the magnetization direction $\tilde{\mathbf{m}}$ in the rotating frame $(\tilde{x}, \tilde{y}, \tilde{z})$ is given by [14]

$$\frac{d\tilde{\mathbf{m}}}{d\tau} = -\tilde{\mathbf{m}} \times [h_{\text{rf}}\mathbf{e}_{\tilde{x}} + (-h_z + \tilde{m}_{\tilde{z}} - \omega_{\text{rf}})\mathbf{e}_{\tilde{z}}] + \alpha\omega_{\text{rf}}\tilde{\mathbf{m}} \times \mathbf{e}_{\tilde{z}} + \alpha\tilde{\mathbf{m}} \times \frac{d\tilde{\mathbf{m}}}{d\tau}. \quad (2)$$

Note that the damping constant α is the only remaining parameter as a result of the normalization.

Figures 7(a) and 7(b) show the cone angle of the steady-state solutions obtained by setting $d\tilde{\mathbf{m}}/d\tau=0$ and analytically solving Eq. (2). The stability of the solution—stable, saddle, and unstable—evaluated by introducing a small deviation is also shown. Parameters $\alpha = 0.17$ and $h_{\text{rf}} = 0.05$ are chosen to reproduce the experimentally obtained CF- and VF-MAS results for $V_{\text{rf}} = 1.0$ V, which we discuss later in detail. For clarity, the cone angle is shown up to 90° , and there is always a stable state near 180° , which corresponds to the switched state. Here, stable state

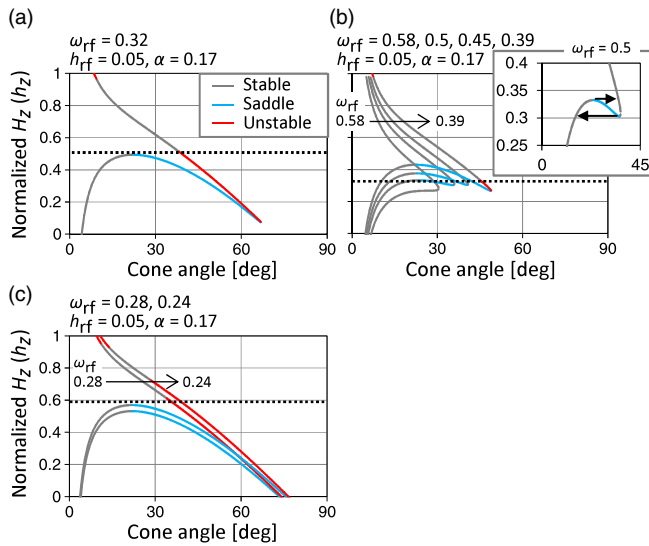


FIG. 7. (a) Cone angle and stability of the magnetization excitation for $h_z = 0.05$ and $\alpha = 0.17$ at the critical frequency ($\omega_{\text{rf}} = 0.32$), (b) at higher ω_{rf} values, and (c) at lower ω_{rf} values. In (b), ω_{rf} is 0.58, 0.5, 0.45, and 0.39 from the curve with the smallest cone angle to the one with the largest cone angle. (Inset) An enlarged view of the data for $\omega_{\text{rf}} = 0.5$. In (c), ω_{rf} is 0.28 and 0.24 from the curve with the smaller cone angle to the one with the larger cone angle.

means that the magnetization can stay in the state and rotates in synchronization with the microwave field. The magnetization cannot stay in unstable and saddle states and move to the stable state. Figure 7(a) corresponds to the critical frequency ($\omega_{\text{rf}} = 0.32$) for CF MAS. As h_z increases from zero, the magnetization follows the line of the stable state and the cone angle gradually increases because h_z approaches the resonance condition. At around $h_z = 0.5$ (the dashed line), the stable state disappears, which means that the induced magnetization excitation overcomes the barrier for switching. Thus, the magnetization moves to the other stable state near 180° , and MAS occurs. The solution shows hysteresis like a protrusion toward the lower-right direction. In CF MAS, however, this hysteresis is saddle or unstable and has no effect on magnetization switching.

Figure 7(b) shows calculation results for ω_{rf} values higher than the critical frequency. At $\omega_{\text{rf}} = 0.58$, a peak appears in the cone angle due to FMR. As ω_{rf} decreases to 0.5, hysteresis appears and two stable states exist in a narrow h_z range near 0.3. These two stable states are referred to as a lower-angle branch and higher-angle branch. As shown in the inset of Fig. 7(b), the magnetization follows the higher-angle branch in the downward h_z sweep, and the cone angle abruptly decreases at the edge of the higher-angle branch. Similarly, the magnetization follows the lower-angle branch in the upward h_z sweep, and the cone angle abruptly increases at the edge of the lower-angle branch. This is called the fold-over effect [23]. In the experiments, h_z is swept only in the upward direction. Thus, in CF MAS where ω_{rf} is fixed, the magnetization is always on the lower-angle branch. At $\omega_{\text{rf}} = 0.45$, this hysteresis becomes more obvious. In these three conditions, MAS does not occur because one or more stable states exist. At $\omega_{\text{rf}} = 0.39$, an unstable state appears around the edge of the higher-angle branch. In CF MAS, this condition is still higher than the critical frequency, and magnetization switching does not occur because of one or more stable states. As seen in Fig. 7(a), this unstable state expands as ω_{rf} further decreases. Now we apply a varying-frequency microwave field. In the experiments, f_{rf} is changed on the nanosecond timescale, while H_z is changed on the second timescale. Therefore, we consider that the magnetization moves on the curves for different ω_{rf} values at constant h_z . As the magnetization moves from a higher ω_{rf} to a lower one, the magnetization is able to stay on the higher-angle branch, which is in contrast to CF MAS, where the magnetization is always on the lower-angle branch. When the higher-angle branch becomes unstable at $\omega_{\text{rf}} = 0.39$, the magnetization can move to the stable state near 180° instead of the stable lower-angle branch, which results in the enhanced MAS by a varying-frequency microwave field.

The unstable state in the higher-angle branch appears when ω_{rf} is slightly higher than the critical frequency,

which indicates that ω_{rf} needs to decrease to a slightly higher value than the critical frequency to induce VF MAS. This result explains the experimentally obtained dependence on $f_{\text{rf}}^{\text{end}}$ [Fig. 4(e)], in which the MAS effect appears when $f_{\text{rf}}^{\text{end}}$ is almost the same as or lower than the critical frequency. The dependence on $f_{\text{rf}}^{\text{start}}$ can be explained by using Figs. 7(a) and 7(b). The switching condition for CF MAS is determined by the edge of the lower-angle branch, where the stable state disappears. In VF MAS, the cone angle first increases at the edge of the lower-angle branch. As f_{rf} decreases, the magnetization stays on the higher-angle branch until it becomes unstable. In other words, both CF and VF MAS are initiated by the transition of the magnetization excitation at the edge of the lower-angle branch. Because this edge shows an almost linear relationship with respect to ω_{rf} , the H_{sw} curves for CF and VF MAS show the same linear relationship with respect to $f_{\text{rf}}^{\text{const}}$ and $f_{\text{rf}}^{\text{start}}$, regardless of the fact that magnetization switching occurs in a different manner.

The dependence on the rate of f_{rf} change can be understood as follows. When ω_{rf} changes fast, the cone angle of the magnetization becomes smaller than the calculated value because the calculated value is a steady-state solution and f_{rf} changes faster than the relaxation time of the magnetization. When the magnetization cannot keep staying on the higher angle branch and falls to the lower-angle branch, MAS cannot be enhanced. As shown in Fig. 6(c), even when the rate of f_{rf} change becomes so fast that the enhancement of MAS disappears, H_{sw} is still smaller than the intrinsic H_{sw} . In this condition, MAS occurs when f_{rf} decreases below the critical frequency. This result indicates that this kind of MAS in which f_{rf} changes below the critical frequency occurs for faster f_{rf} change relative to the enhancement of MAS in which f_{rf} changes above the critical frequency. This difference can be explained as follows. Figure 7(c) shows calculation results for ω_{rf} values slightly lower than the critical frequency. At around $h_z = 0.6$ (the dashed line) there is no stable state for either $\omega_{\text{rf}} = 0.28$ or 0.24 . When ω_{rf} changes in this range, the magnetization moves one way to the switched state. In contrast, when ω_{rf} is higher than the critical frequency, the magnetization can fall from the higher-angle branch to the lower-angle branch during the ω_{rf} change. Because the magnetization moves one way to the switched state during the ω_{rf} change, this kind of MAS occurs when the rate of f_{rf} change is relatively fast.

The minimum switching h_z obtained for VF MAS is 0.33, as indicated by the dashed line in Fig. 7(b). This h_z corresponds to the limit where the higher-angle branch always exists during the f_{rf} change, which is necessary for the cone angle to gradually increase until switching occurs.

We compare the experimental results with the calculation, and for this purpose, we estimate the H_{sw} value without microwave fields as follows. The intrinsic H_{sw} of 5.7 kOe reflects thermally activated magnetization

switching. Although MAS is also thermally activated, the thermal effect acts effectively only during the microwave field application, which has a duty ratio of approximately 0.001 (10-ns plateau time and 122-kHz repetition). Owing to the difference in the timescale of thermal effect, MAS above the intrinsic H_{sw} is screened, and the H_{sw} versus $f_{\text{rf}}^{\text{const}}$ curves change a slope at around $f_{\text{rf}}^{\text{const}} = 3$ GHz in Fig. 3(a). If the thermal effect were reduced to that of the timescale of MAS, the H_{sw} versus $f_{\text{rf}}^{\text{const}}$ curves would have a constant slope and the intercept at $f_{\text{rf}}^{\text{const}} = 0$ Hz would be H_{sw} in the static in-plane field with an amplitude of H_{rf} . Thus, the intercept of the extrapolated H_{sw} versus $f_{\text{rf}}^{\text{const}}$ curve for $V_{\text{rf}} = 0.5$ V, which is approximately 7 kOe, is employed as the H_{sw} with no microwave field under the reduced thermal effect. The ratios of the minimum H_{sw} for $V_{\text{rf}} = 1.0$ V obtained by CF and VF MAS [3.8 kOe in Fig. 3(b) and 2.6 kOe in Fig. 5] to this H_{sw} value are 0.54 and 0.37, respectively, which approximately coincides with the calculation results of 0.5 and 0.33.

We would like to comment on α and the microwave field amplitude. The damping parameter $\alpha = 0.17$ is larger than the value estimated from the VNA-FMR measurement of the film. This deviation may originate from the fact that MAS involves large-amplitude magnetization excitation, whereas the VNA-FMR measurement uses small-amplitude magnetization precession. Increase of α by a factor of 5 in large-amplitude magnetization excitation has been reported [24]. In addition, α is affected by the fact that the nanomagnet has a nonuniform demagnetizing field, whereas the film has a uniform demagnetizing field. When we use the H_{sw} of 7 kOe without a microwave field as H_{ani} for a rough estimation, $h_{\text{rf}} = 0.05$ corresponds to $H_{\text{rf}}^{\text{rot}} = 350$ Oe for a rotating microwave field and $H_{\text{rf}} = 700$ Oe for an alternating microwave field, which is much larger than $H_{\text{rf}} = 85$ Oe in the experiments. This disagreement is because of the fact that the calculation does not include thermal activation and spatially nonuniform magnetization excitation. According to the study using a macrospin model with thermal activation [14], thermal effects alone cannot explain the disagreement, and spatially nonuniform magnetization excitation may make a large contribution. The issue of nonuniform magnetization excitation is presented in Ref. [6], which discusses a comparison of experimental results, macrospin simulations, and micromagnetic simulations.

Figures 8(a) and 8(b) show the calculation results for $h_{\text{rf}} = 0.075$. Similar to the case of $h_{\text{rf}} = 0.05$, enhancement of the MAS effect by a varying-frequency microwave field appears. According to this approach, the enhancement of the MAS effect becomes larger as h_{rf} increases, which cannot explain the experimental result in which the enhancement of the MAS effect is the largest for $V_{\text{rf}} = 1.0$ V. Because α is the only parameter in Eq. (2), the experimental result can be understood as increased

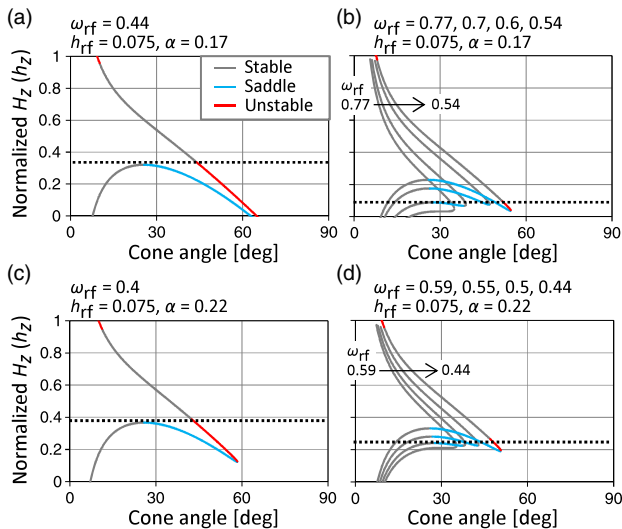


FIG. 8. (a),(b) Cone angle and stability of the magnetization for $h_z = 0.075$ and $\alpha = 0.17$ at the critical frequency ($\omega_{rf} = 0.44$) and at higher ω_{rf} values. In (b), ω_{rf} is 0.77, 0.7, 0.6, and 0.54 from the curve with the smallest cone angle to the one with the largest cone angle. (c),(d) Cone angle and stability of the magnetization for $h_z = 0.075$ and $\alpha = 0.22$ at the critical frequency ($\omega_{rf} = 0.4$) and at higher ω_{rf} values. In (d), ω_{rf} is 0.59, 0.55, 0.5, and 0.44 from the curve with the smallest cone angle to the one with the largest cone angle. The dashed lines show the minimum switching h_z for CF and VF MAS.

damping in large magnetization excitation. As shown in Figs. 8(c) and 8(d), the hysteresis becomes less evident as α is increased to 0.22. Because CF MAS does not utilize the hysteresis, the MAS effect of CF MAS is almost unchanged. However, because VF MAS utilizes the hysteresis, the enhancement of the MAS effect by VF MAS decreases as α increases. This α dependence is consistent with previous theoretical and simulation studies [16,20]. This result implies that the effective damping of the nanomagnet may increase as the magnetization excitation becomes larger, which reduces the enhancement of the MAS effect in a varying-frequency microwave field. The effective damping includes the intrinsic damping of the material, the spatial inhomogeneity of the magnetic anisotropy and the demagnetizing field, the spatially nonuniform magnetization excitation, and the spin pumping.

V. SUMMARY

In this paper, we study the switching of a perpendicularly magnetized nanomagnet in a microwave field with time-varying frequency and explain the switching behavior by using the theory based on the macrospin model. When the frequency of the microwave field gradually decreases, a larger MAS effect than that in a constant-frequency microwave field is obtained because the microwave field frequency follows the nonlinear decrease of the resonance

frequency and induces larger magnetization excitation. The switching field decreases almost linearly as the start frequency of the microwave field increases up to a certain frequency, beyond which further increases in the start frequency do not change the switching field. To obtain enhancement of the MAS effect, the end frequency of the microwave field needs to be approximately the same as or lower than the critical frequency for constant-frequency MAS. In addition, frequency change of a microwave field needs to take approximately 1 ns to make the rate of change sufficiently slow that the magnetization excitation can follow the varying-frequency microwave field.

ACKNOWLEDGMENTS

We thank Canon ANELVA Corp. for the technical support. This work was supported by Strategic Promotion of Innovative Research and Development from the Japan Science and Technology Agency, JST.

- [1] C. Thirion, W. Wernsdorfer, and D. Mailly, Switching of magnetization by non-linear resonance studied in single nanoparticles, *Nat. Mater.* **2**, 524 (2003).
- [2] J.-G. Zhu, X. Zhu, and Y. Tang, Microwave assisted magnetic recording, *IEEE Trans. Magn.* **44**, 125 (2008).
- [3] J.-G. Zhu and Y. Wang, Microwave assisted magnetic recording utilizing perpendicular spin torque oscillator with switchable perpendicular electrodes, *IEEE Trans. Magn.* **46**, 751 (2010).
- [4] I. Tagawa, M. Shiimoto, M. Matsubara, S. Nosaki, Y. Urakami, and J. Aoyama, Advantage of MAMR read-write performance, *IEEE Trans. Magn.* **52**, 3101104 (2016).
- [5] S. Okamoto, N. Kikuchi, M. Furuta, O. Kitakami, and T. Shimatsu, Microwave assisted magnetic recording technologies and related physics, *J. Phys. D* **48**, 353001 (2015).
- [6] M. Furuta, S. Okamoto, N. Kikuchi, O. Kitakami, and T. Shimatsu, Size dependence of magnetization switching and its dispersion of Co/Pt nanodots under the assistance of radio frequency fields, *J. Appl. Phys.* **115**, 133914 (2014).
- [7] H. Suto, T. Nagasawa, K. Kudo, T. Kanao, K. Mizushima, and R. Sato, Layer-Selective Switching of a Double-Layer Perpendicular Magnetic Nanodot Using Microwave Assistance, *Phys. Rev. Applied* **5**, 014003 (2016).
- [8] S. Okamoto, N. Kikuchi, and O. Kitakami, Magnetization switching behavior with microwave assistance, *Appl. Phys. Lett.* **93**, 102506 (2008).
- [9] H. Suto, T. Kanao, T. Nagasawa, K. Kudo, K. Mizushima, and R. Sato, Subnanosecond microwave-assisted magnetization switching in a circularly polarized microwave magnetic field, *Appl. Phys. Lett.* **110**, 262403 (2017).
- [10] T. Taniguchi, D. Saida, Y. Nakatani, and H. Kubota, Magnetization switching by current and microwaves, *Phys. Rev. B* **93**, 014430 (2016).
- [11] H. Suto, T. Kanao, T. Nagasawa, K. Mizushima, and R. Sato, Zero-dc-field rotation-direction-dependent magnetization switching induced by a circularly polarized microwave magnetic field, *Sci. Rep.* **7**, 13804 (2017).

- [12] G. Bertotti, C. Serpico, and I.D. Mayergoyz, Nonlinear Magnetization Dynamics under Circularly Polarized Field, *Phys. Rev. Lett.* **86**, 724 (2001).
- [13] T. Taniguchi, Magnetization reversal condition for a nanomagnet within a rotating magnetic field, *Phys. Rev. B* **90**, 024424 (2014).
- [14] H. Suto, K. Kudo, T. Nagasawa, T. Kanao, K. Mizushima, R. Sato, S. Okamoto, N. Kikuchi, and O. Kitakami, Theoretical study of thermally activated magnetization switching under microwave assistance: Switching paths and barrier height, *Phys. Rev. B* **91**, 094401 (2015).
- [15] K. Rivkin and J. B. Ketterson, Magnetization reversal in the anisotropy-dominated regime using time-dependent magnetic fields, *Appl. Phys. Lett.* **89**, 252507 (2006).
- [16] S. Okamoto, N. Kikuchi, and O. Kitakami, Frequency modulation effect on microwave assisted magnetization switching, *Appl. Phys. Lett.* **93**, 142501 (2008).
- [17] Z. Wang and M. Wu, Chirped-microwave assisted magnetization reversal, *J. Appl. Phys.* **105**, 093903 (2009).
- [18] T. Taniguchi, Magnetization switching by microwaves synchronized in the vicinity of precession frequency, *Appl. Phys. Express* **8**, 083004 (2015).
- [19] K. Kudo, H. Suto, T. Nagasawa, K. Mizushima, and R. Sato, Resonant magnetization switching induced by spin-torque-driven oscillations and its use in three-dimensional magnetic storage applications, *Appl. Phys. Express* **8**, 103001 (2015).
- [20] T. Yamaji, H. Arai, R. Matsumoto, and H. Imamura, Critical damping constant of microwave-assisted magnetization switching, *Appl. Phys. Express* **9**, 023001 (2016).
- [21] S. I. Kiselev, J. C. Sankey, I. N. Krivorotov, N. C. Emley, R. J. Schoelkopf, R. A. Buhrman, and D. C. Ralph, Microwave oscillations of a nanomagnet driven by a spin-polarized current, *Nature (London)* **425**, 380 (2003).
- [22] D. Houssameddine, U. Ebels, B. Delaet, B. Rodmacq, I. Firastrau, F. Ponthenier, M. Brunet, C. Thirion, J.-P. Michel, L. Perjbeanu-Buda, M.-C. Cyrille, O. Redon, and B. Dieny, Spin-torque oscillator using a perpendicular polarizer and a planar free layer, *Nat. Mater.* **6**, 447 (2007).
- [23] P. W. Anderson and H. Suhl, Instability in the motion of ferromagnets at high microwave power levels, *Phys. Rev.* **100**, 1788 (1955).
- [24] Th. Gerrits, M. L. Schneider, A. B. Kos, and T. J. Silva, Large-angle magnetization dynamics measured by time-resolved ferromagnetic resonance, *Phys. Rev. B* **73**, 094454 (2006).